Romanian Reports in Physics, Vol. 64, No. 1, P. 325–333, 2012

SEARCH FOR NUCLEARITES WITH THE ANTARES DETECTOR*

GABRIELA EMILIA PĂVĂLAŞ

Institute for Space Science, Atomistilor 409, PO Box Mg-23, Magurele, Ro 077125, Ilfov, Romania
E-mail: gpavalas@spacescience.ro

Received November 20, 2010

Abstract. ANTARES is an underwater detector in the Mediterranean Sea, dedicated to the search for cosmic neutrinos. While it is optimized to detect the Cherenkov signal from up-going relativistic particles, ANTARES could also observe slow massive exotic objects. In this report we discuss the detection of down-going nuclearites with the ANTARES telescope in the 12 line configuration, and present a preliminary flux upper limit for these particles using a set of data from 2008.

Key words: ANTARES detector-nuclearites.

1. INTRODUCTION

The main goal of the ANTARES neutrino telescope is to detect high energy neutrinos from galactic and extragalactic sources, such as supernovae, binary systems and gamma ray bursts. The detector is optimized to collect the Cherenkov light emitted by up-going relativistic muons, produced in neutrino interactions below the detector.

ANTARES detector may be also sensitive to heavy exotic particles, such as nuclearites [1, 2]. Nuclearites are hypothetical lumps of strange quark matter that could be present in cosmic radiation, with characteristic velocities of ~ 300 km/s. They may be formed in the Early Universe or as debris from supernovae and strange stars collisions. Cosmic nuclearites will transfer some of their energy as visible light, while traversing transparent media (water, air). The goal of the present analysis is to determine a preliminary upper limit of the nuclearite flux.

* Paper presented at the Annual Scientific Session of Faculty of Physics, University of Bucharest, June 18, 2010, Bucharest-Măgurele, Romania.

2. THE ANTARES DETECTOR

The ANTARES detector is located on the floor of the Mediterranean Sea, at a depth of 2.5 km, near Toulon, France. It consists of a large number of photomultiplier tubes (PMTs) placed on 12 lines anchored on the seabed. The detector is operated from a control room on shore.

The sensitive element of the ANTARES telescope is a hemispherical 10" Hamamatsu photomultiplier tube, housed in a pressure resistant glass sphere [3]. A triplet of PMTs forms a storey, together with the read-out and control electronics. A detector line has a length of 450 m and contains 25 storeys, distributed at every 14.5 m, starting 100 m above the seabed. Every line is connected to a Junction Box, itself connected to the shore station at La Seyne-sur-Mer through a 40 km long electro-optical cable.

The 885 PMTs of the ANTARES detector in the 12 line configuration form a 3 dimensional array that instruments a surface area of about 0.1 km^2. The PMT signals larger than a preset threshold (0.3 photoelectrons) are digitized and the corresponding time and charge information (referred to as L0 hits) are sent to shore. The data are processed by a computer farm at the shore station, using different triggers for physics signals [4].

For the analysis presented here, two muon triggers have been considered, that are based on L1 hits. A L1 hit is defined either as a local coincidence on the same storey within 20 ns, or as a single L0 hit with a large amplitude, typically 3 photoelectrons. The so-called 3N muon trigger requires five local coincidences causally connected, within a time window of 2.2 μs, while the T3 muon trigger requires two coincidences between two L1 hits in adjacent or next-to-adjacent storeys. When a muon event is triggered, all PMT pulses are recorded over 4 μs in a snapshot.

The ANTARES observatory was taking data in partial configurations since March 2006, and was completed with 12 lines in May 2008. First results are presented in [5, 6].

3. NUCLEARITES

Proposed by Witten [7] and De Rujula [8], nuclearites would be stable particles of strange quark matter, with an energy density slightly higher than the ordinary matter. They would have typical galactic velocities of $\sim 10^{-3}c$ and would interact with the surrounding medium *via* elastic and quasi-elastic collisions, with an energy loss:

$$\frac{\mathrm{d}E}{\mathrm{d}x} = -\sigma\rho v^2,$$

where ρ is the density of the medium, v is the nuclearite velocity and σ its geometrical cross section:

$$\sigma = \begin{cases} \pi(3M / 4\pi\rho_N)^{2/3} & \text{for } M \geq 8.4\times10^{17} \text{ GeV}; \\ \pi\times10^{-16}\,\mathrm{cm}^2 & \text{for smaller masses}, \end{cases}$$

with $\rho_N \approx 3.6\times10^{14}$ g·cm^{-3}.

Nuclearites moving slowly through water would produce a thermal shock emitting blackbody radiation. The luminous efficiency in water was estimated to be $\eta \approx 3\times10^{-5}$ by [8] and the number of visible photons emitted per unit path length can be computed as follows:

$$\frac{\mathrm{d}N_\gamma}{\mathrm{d}x} = \eta\frac{\mathrm{d}E/\mathrm{d}x}{\pi(\mathrm{eV})},$$

assuming a mean energy of visible photons of π eV. We show in Fig.1 the number of photons per unit path length emitted by nuclearites with the velocity $\beta = 10^{-3}$, for the 10^{13}–10^{18} GeV mass range.

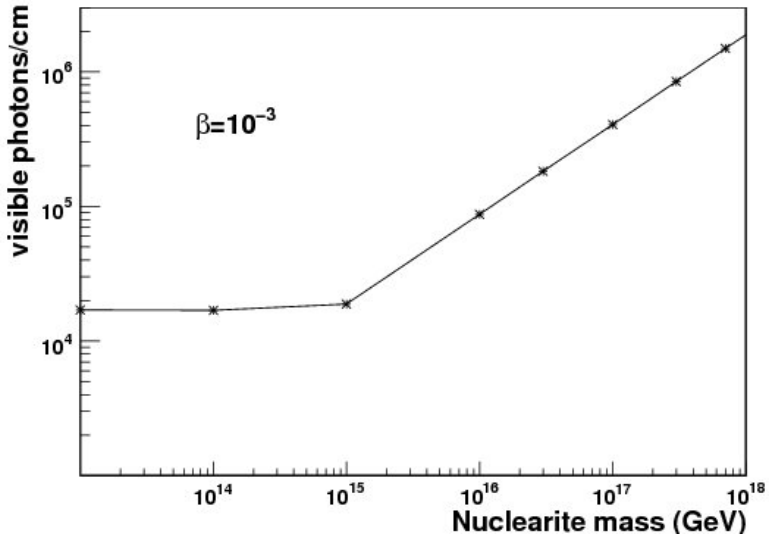

Fig. 1 – Number of photons per unit path length produced by nuclearites, considering the velocity $\beta = 10^{-3}$ for all masses.

4. SEARCH STRATEGY AND RESULTS

The Monte Carlo simulations of nuclearite events in Antares consider as generation volume a hemisphere of 548 m radius, that surrounds symmetrically the detector. The initial point of the trajectory and the direction of the nuclearite are randomly generated. The algorithm proceeds in steps of 2 ns, evaluating the position and β of nuclearites, as well as the number of hits on the PMTs.

We have simulated down-going nuclearites in the 12 line configuration, with an initial velocity (before entering the atmosphere) of $\beta = 10^{-3}$ and a nuclearite mass range from 10^{15} to 10^{18} GeV .

A typical nuclearite would cross the Antares detector in a characteristic time of ~ 1 ms, producing a light signal that would exceed that of muons by several orders of magnitude. Down-going atmospheric muons represent the main background for nuclearites. The atmospheric muons were generated with the MUPAGE code [9], considering an energy range from 20 GeV to 500 TeV.

We used in our analysis a set of data taken in the 12 line configuration, from May to December 2008. The selected data set satisfies certain quality criteria, such as a baseline rate less than 120 kHz and a burst fraction (due to bioluminiscence) less than 40%. The light produced by the organisms living in the sea also contributes to the background noise in the apparatus.

Two high thresholds were used for data acquisition in 2008, 10 and 3 photoelectrons, as well as the two trigger types described in the Section 2, see Table 1.

Table 1

Trigger types, thresholds and active time for 12 line data taken in 2008

Trigger	Active time
3N, T3, 10 pe	27.3 days
3N, T3, 3 pe	42.8 days

The simulated nuclearites and atmospheric muons were processed with the 3N and T3 muon triggers, and background noise was added from a selection of runs.

We found that the lower detectable nuclearite mass with both 3N and T3 triggers is 10^{15} GeV. Due to the fact that nuclearites are slowly moving particles, both the 3N and T3 trigger may record more consecutive snapshots corresponding to a single nuclearite event.

The T3 trigger is much more efficient than the 3N trigger for nuclearites, due to the less restrictive selection conditions. For example, when 3N and T3 triggers are applied simultaneously on the nuclearite sample of 10^{18} GeV mass, about 82% of the snapshots are produced by the T3 trigger.

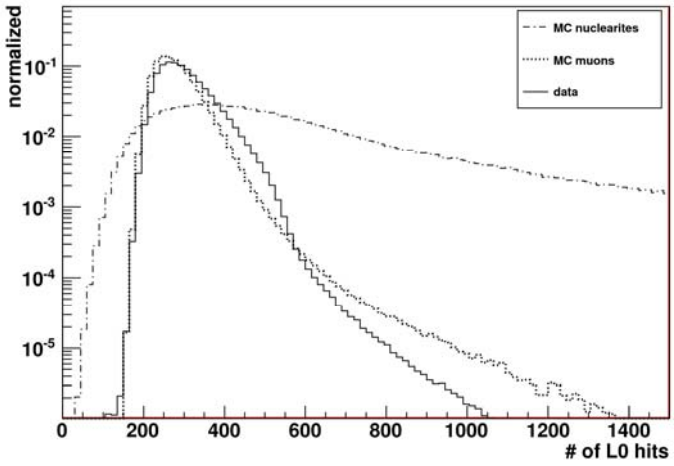

Fig. 2 – Normalized distributions of the number of L_0 hits/per snapshot for simulated nuclearites (dash-dot line), muon events (dotted line) and experimental data (continuous line).

In order to define selection criteria for the nuclearite signal, we studied several parameters at the trigger level. These are the number of L1 hits (see Section 2), the number of single hits (L0 hits, defined as hits with a threshold greater than 0.3 photoelectrons), and the duration of the L1 cluster (defined as the time difference between the last and the first L1 hits of a snapshot), where a snapshot contains all the hits from a muon triggered event.

In the following, we compare parameter distributions, normalized to 1, for simulated nuclearites, atmospheric muons and data taken with 12 lines in 2008, at 3 pe high threshold.

The distributions of the number of L0 hits per snapshot are represented in Fig. 2, for simulated nuclearites (dash-dot line), muons (dotted line) and data (continuos line). We observe a significant excess of L0 hits for the nuclearite distribution, that makes this parameter a good discriminative variable. The data-MC muons agreement is relatively good, with some discrepancy at the tail of the distributions.

The distributions of the number of L1 hits per snapshot are shown in Fig. 3, for simulated nuclearites (dash-dot line), muons (dotted line) and data (continuos line). An excess of L1 hits for the nuclearite distribution is also seen.

The last parameter studied is the duration of the L1 cluster, shown in Fig. 4. The longer duration of the L1 cluster for nuclearite snapshots is due to their larger light output.

The sharp cut at 2 200 ns in dt distributions of Fig. 4 is due to the condition in the T3 trigger that defines the maximum time window of a relativistic particle in

the detector. Nuclearites produce a long trail of light in the detector spanned over hundreds of microseconds to few milliseconds, seen as a series of connected snapshots.

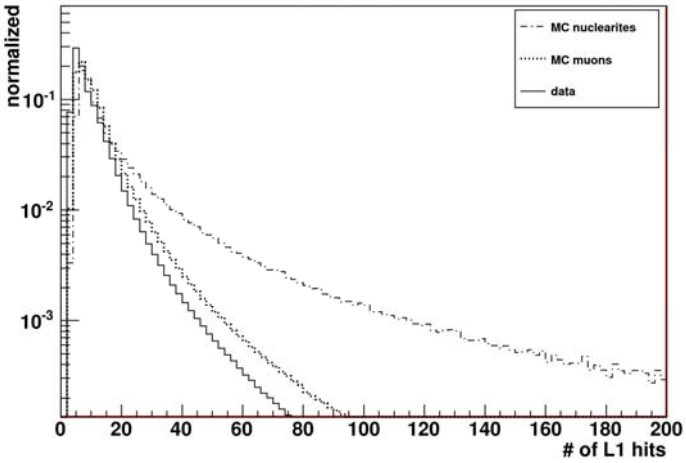

Fig. 3 – Normalized distributions of the number of L_1 hits/per snapshot for simulated nuclearites (dash-dot line), muon events (dotted line) and experimental data (continuous line).

We tested several cuts on MC samples and data using individual parameters, that provided a good efficiency for nuclearite events, but a less efficient noise rejection. We also tested some cuts using linear combinations of parameters, and found a linear cut using the number of L1 hits and L0 hits that gives a better noise rejection efficiency.

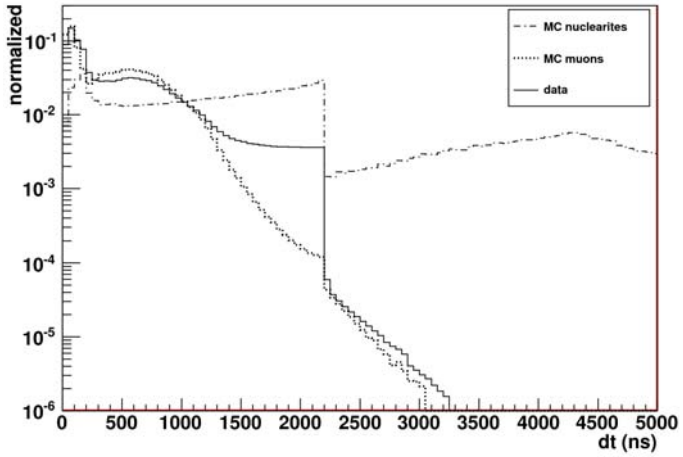

Fig. 4 – Normalized distributions of the L1 cluster duration (dt) for simulated nuclearites (dash-dot line), muon events (dotted line) and experimental data (continuous line).

So, we defined the first cut (C1) as L1 < 0.245×L0-276.9, as well as a second cut (C2), that requires two consecutive triggered snapshots in less than 1 ms, the so-called multiple snapshot cut. A similar search strategy for nuclearites was presented in [2].

The efficiencies of the two cuts on MC nuclearites are given in Table 2, for the mass range 10^{15}–10^{18} GeV in the 12 line configuration. After applying the cuts on nuclearite events, only events with mass higher or equal to 10^{16} GeV remain.

In case of the 12 line data, 2 events remain for data taken at 10 pe high threshold and none for data taken at 3 pe threshold, which gives a rejection efficiency of the two cuts of practically 100%. The events remaining in data are related to the biological environmental activity and are considered as backgound.

Table 2

Efficiencies of the linear and multiple snapshot cuts for nuclearite samples

Nuclearite sample	MC triggered events	C1 efficiency	C1 & C2 efficiency
12 lines, 10 pe	25974	60.9%	54.7%
12 lines, 3 pe	28049	64.4%	52.2%

The 90% C.L. flux upper limits are calculated with the Feldman-Cousins formula [10], considering events with a Poisson distribution:

$$\phi_{90} = \frac{\mu_{90}}{A \times T},$$

where μ_{90} is a function of the number of observed events and of the expected background, taken from the Feldman-Cousins tables, A is the detector acceptance, and T is the active time corresponding to data taken at 3 pe and 10 pe thresholds.

The effective acceptance A of ANTARES to a down-going flux of nuclearites is computed for each mass as follows:

$$A = 2\pi \times S \times \frac{N_{nucl}}{N_{sim}},$$

where S is the area of the hemisphere and $\frac{N_{nucl}}{N_{sim}}$ is the ratio of the number of nuclearite events that passed the selection cuts to the number of simulated events.

The flux upper limits for nuclearites are computed for the active periods of the 12 line ANTARES data taken at 10 pe and 3 pe high thresholds, for no observed signal. Since the results obtained for each threshold are independent, we determined a preliminary global upper limit for the nuclearite flux using the 12 line data, as shown in Fig. 5. We also represented the upper limits obtained by two experiments that were searching for nuclearites. One of them is MACRO [11], an

underground detector at Gran Sasso, in Italy, that took data for about 8 years and the other one is SLIM [12], an experiment using plastic nuclear track detectors at high altitude, in Bolivia.

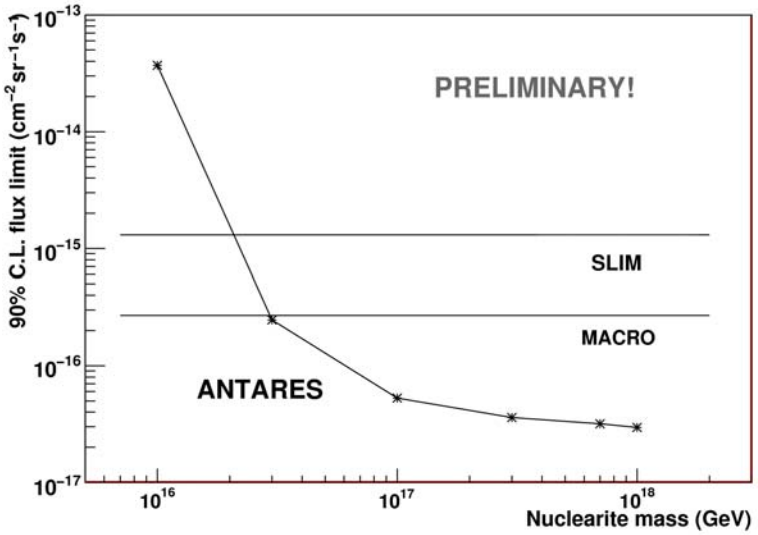

Fig. 5 – Flux upper limit for down-going nuclearites using ~ 70 days of data taken with ANTARES detector in 12 line configuration in 2008.

This result shows that the ANTARES detector is sensitive to massive exotic particles, even in the absence of a dedicated trigger. The global flux upper limit for down-going nuclearites obtained with the 12 line data set improves the MACRO result by more than a factor 5 for nuclearite masses greater than 10^{17} GeV.

5. CONCLUSIONS

We presented a search strategy and a preliminary flux upper limit for non-relativistic nuclearites using a set of 12 line ANTARES data. The flux upper limit for this configuration of the ANTARES detector improves the upper limit for heavy nuclearites obtained by the MACRO experiment.

REFERENCES

1. V. Popa, Nucl. Instrum. Meth., **A567**, 480 (2006).
2. G. Pavalas, N. Picot-Clemente, Proceedings of the 31st ICRC, Lodz 2009, arXiv:0908.0860.
3. J. A. Aguilar et al. (ANTARES Collaboration), Nucl. Instrum. Meth., **A555**, 132 (2005).
4. J. A. Aguilar et al. (ANTARES Collaboration), Nucl. Instrum. Meth., **A570**, 107 (2007).

5. M., Ageron et al. (ANTARES Collaboration), Astropart. Phys., **31**, 277 (2009).
6. J.A., Aguilar et al. (ANTARES Collaboration), to be published in Astropart. Phys.
7. E., Witten, Phys. Rev., **D30**, 272 (1984).
8. A., De Rujula, S.L., Glashow, Nature, **312**, 734 (1984).
9. G., Carminati et al., Computer Physics Communications, **179**, 915 (2008).
10. G.J., Feldman, R.D., Cousins, Phys. Rev., **D57**, 3873 (1998).
11. M., Ambrosio et al., (MACRO Collaboration), Eur. Phys. J., **C26**, 163 (2002);
G., Giacomelli and L., Patrizii, hep-ex/0506014.
12. S., Cecchini et al, Eur. Phys. J., **C57**, 525 (2008);
Z. Sahnoun for the SLIM Collaboration, Radiat. Meas., **44**, 894 (2009).